Drug Design, Development and Therapy

Dovepress
open access to scientific and medical research

Open Access Full Text Article

ORIGINAL RESEARCH

Development of dual delivery antituberculotic system containing rifapentine microspheres and adipose stem cells seeded in hydroxyapatite/tricalcium phosphate

This article was published in the following Dove Medical Press journal:
Drug Design, Development and Therapy

Qiuzhen Liang
Xinghua Song
Shengli She
Zhen Wang
Chong Wang
Dawei Jiang

Department of Orthopaedics, The First Affiliated Hospital of Xinjiang Medical University, Urumqi 830054, China

Background: Low drug concentration in the tuberculosis (TB) lesion and bone defects or nonunion after debridement are two major problems that occur in the course of treating osteoarticular TB. Thus, the combination of drug-delivery system and bone tissue repair appears to be the most promising option for osteoarticular TB treatment.

Materials and methods: Herein, we report a novel anti-TB dual delivery system based on rifapentine polylactic acid microspheres (RPMs) to treat infections, with the addition of adipose-derived mesenchymal stem cells (ASCs) seeded in hydroxyapatite/tricalcium phosphate (HA/TCP) to promote bone formation. Cell proliferation, osteogenesis, and apoptosis were performed to investigate the effects of rifapentine on ASCs. The RPMs were synthesized by emulsion-solvent evaporation method, and then the monolayer composite (ASC + RPM) and three-dimensional (3D) composite scaffold (ASC + RPM + HA/TCP) were constructed, respectively. The alkaline phosphatase (ALP) activity and real-time PCR were used for determining the osteogenic differentiation. The concentrations of rifapentine resulting from the composites were detected.

Results: The results showed that rifapentine has no influence on ASCs proliferation and osteogenesis when the drug concentration was below 20 μg/mL, which was significantly higher than minimal inhibitory concentration. The drug loading and encapsulation efficiency of RPMs were 40.56%±2.63% and 70.24%±2.18%, respectively. The proliferation of the cells in monolayer was higher than that in 3D composite, and the addition of RPMs slightly increased the proliferation. The ALP activity and gene expression of osteocalcin and osteopontin were higher in the 3D composite than those in the monolayer. Good biocompatibility was observed by microscopic image and H&E stain. The release tests revealed that the 3D composite exhibited sustained release profiles of rifapentine for 76 days. The dual delivery systems in 3D composite could moderate the burst release and extend the length of release time when compared to single delivery in monolayers.

Conclusion: In conclusion, such dual delivery antituberculotic scaffold represents a potential new strategy for TB infections and bone defects.

Keywords: tuberculosis, rifapentine, drug delivery, release system, scaffold, tissue engineering

Correspondence: Xinghua Song
Department of Orthopaedics, The First Affiliated Hospital of Xinjiang Medical University, No 137, Liyushan South Road, Urumqi 830054, Xinjiang, China
Email 811789561@qq.com

Introduction

Tuberculosis (TB) caused by *Mycobacterium tuberculosis* is one of the most fatal infectious diseases. It is more prevalent in poor and under-developed countries, especially in Africa and the South-East Asian region, and is responsible for 1.5 million deaths

annually.[1] Osteoarticular TB accounts for 35% of extrapulmonary TB.[2] Low drug concentration in the TB lesion and bone defects or nonunion after debridement are two major problems that occur in the course of treating osteoarticular TB.[3–6] Thus, the combination of a drug-delivery system and a bone tissue repair system appears to be the most promising option for osteoarticular TB treatment. Herein, we report a novel composite scaffold, which allows the controlled release of anti-TB drug and promotes bone formation in local lesions, simultaneously.

At present, the traditional oral anti-TB agents do not result in satisfactory treatment of osteoarticular TB, due to the low drug concentration achieved locally in the TB lesion and a series of side effects.[3,7] The clinical application of anti-TB drugs to local areas has been shown to be effective after the removal of the bone lesion.[8,9] However, because the drugs like streptomycin or isoniazid are highly water soluble, they are dissolved and absorbed quickly after being implanted during surgery. Rifapentine shows adequate fat solubility and antibacterial properties identical to rifampin. Moreover, rifapentine has a greater inhibitory and bactericidal activity against tubercle bacillus, with minimal inhibitory concentration (MIC) of 0.015–0.06 μg/mL.[10,11] Thus, we used rifapentine to construct an anti-TB drug release system, which may play an important role in treating osteoarticular TB by preventing the local lesion from recurring. Based on the solubility and stability of rifapentine, we used the double-emulsion solvent evaporation method for preparing rifapentine polylactic acid sustained-release microspheres (RPMs).

Bone defects are also a problem that occurs in the course of debridement. Thus, the microspheres should be combined with scaffolds to maintain local treatment and mechanical strength. In this study, a three-dimensional (3D) composite scaffold was constructed based on hydroxyapatite/tricalcium phosphate (HA/TCP), which displayed excellent osteoconductive properties.[12] Followed by transplantation for bone defects, bone nonunion is another problem usually due to local recurrence and low osteogenic activity in the transplanted bone. Therefore, we used adipose-derived mesenchymal stem cells (ASCs), which were regarded as one kind of the most promising osteogenic stem cells to promote bone formation.[13]

However, to the best of our knowledge, no previous detailed investigation has evaluated the influence of anti-TB drug on stem cells in the literature. Thus, we cultured the ASCs with varying concentrations of rifapentine to detect the possibility of combination. The results showed that rifapentine has no influence on ASC proliferation and osteogenesis when the concentration of rifapentine was below 20 μg/mL, which was significantly higher than MIC.

In this study, we encapsulated rifapentine in polylactic acid (PLA) microspheres and integrated these microspheres along with ASCs into HA/TCP made of a dual delivery antituberculotic scaffold for bone tissue engineering. We hope this novel composite scaffold could extend the length of release time, helping to fill bone defects and accelerate bone formation.

Materials and methods

Cell isolation and culture

Female New Zealand White rabbits (2.5–3 kg) were obtained from the Animal Center of Xinjiang Medical University. Animal experiments and welfare were complied with the Guide for the Care and Use of Laboratory Animals published by the National Institutes of Health (No 8023), and all experiments were approved by the Ethics Committee of The Xinjiang Medical University (No 20180223–13). In brief, adipose tissue was obtained from inguinal fat pads of rabbits. Samples were washed carefully with PBS to remove debris and red blood cells. Then they were cut into tiny pieces with scissors. Samples were digested in a water bath by using 0.1% collagenase I (Worthington, Lakewood, NJ, USA) and incubating at 37°C for 45 minutes with vigorous shaking. After digestion, collagenase I was neutralized by adding an equal volume of DMEM (Sigma-Aldrich Co.) supplemented with 10% FBS (Sigma-Aldrich Co.). Subsequently, the samples were centrifuged for 10 minutes at 1,200× *g*. Cells were seeded at a density of 10^5 cells/cm^2 and maintained at 37°C in a humidified atmosphere with 5% CO_2. The medium was changed every 2 days. Cells at passage 3 (P3) were harvested for further experiments.

Cell identification

Cell cycle analysis

ASCs at P3 were harvested and fixed in 70% ethanol for 1 day at 4°C. The fixed cells were washed with ice-cold PBS and stained with 50 μg/mL propidium iodide (PI; BD Biosciences, San Jose, CA, USA) at 4°C for 1 hour in the dark. Samples were analyzed by FACS Calibur using Cell Quest software.

Immunofluorescent staining

The P3 ASCs were fixed with 4% formaldehyde, treated with 3% H_2O_2, blocked in 1% BSA, incubated with monoclonal antibodies against CD44 and CD29 (1:1,000 dilution; BD Biosciences) at 4°C overnight, and then incubated with IgG

conjugated with fluorescein isothiocyanate (FITC, 1:200). Fluorescence signals were observed under a fluorescence confocal microscope (IX81; Olympus, Tokyo, Japan).

Adipogenic, osteogenic, and chondrogenic differentiation

The differentiation of ASCs was evaluated using a kit (Saiye Biotech Co. Ltd., Beijing, China). Adipogenic differentiation, osteogeneic differentiation, and chondrogenic differentiation were assessed according to the manufacturer's protocol, followed by Oil Red O staining, Alizarin red staining, and Alcian blue staining, respectively.

Preparation of RPMs

The RPMs were synthesized in our pharmaceutical laboratory, and the antibacterial experiments indicated that RPMs could inhibit the growth of *M. tuberculosis* (National Invention Patent of China (patent number: ZL201210281222.6)). Briefly, PLA (MW 3,000 Da; Jinan Daigang Biotech Co. Ltd., Shandong, China,) was dissolved in dichloromethane, and then rifapentine (lot number: 20100609, content: 93.8%; Sichuan Med-Shine Pharmaceutical Co.Ltd., Sichuan, China) was dissolved into polymer solution. The polymer-solvent-drug solution was uniformly injected into gelatin (G9382; Sigma-Aldrich Co.) for emulsification at room temperature. Subsequently, the emulsion was gently stirred until the DCM volatilized completely. Finally, the RPMs were freeze-dried to obtain free-flowing particles and stored at room temperature. The morphology and size distribution of RPMs were observed under a scanning electron microscope (SEM; JEOL, Tokyo, Japan) at 15 kV. To detect the drug loading and encapsulation efficiency of the RPMs, 5 mg of RPMs was accurately weighed and dissolved in 5 mL of dichloromethane. After incubation for overnight, rifapentine in the solution was detected by UV-visible spectrophotometry (UV-2556; Shimadzu, Kyoto, Japan) at a wavelength of 474 nm.

Influence of rifapentine on ASCs

ASCs were divided into four experimental groups according to the concentration of rifapentine in growth medium: group 1, 0 μg/mL; group 2, 10 μg/mL; group 3, 20 μg/mL; and group 4, 30 μg/mL.

Cell proliferation analysis

To investigate the effects of rifapentine on the proliferation of ASCs, cells were digested, harvested, and seeded in 96-well plates at 5,000 cells/well. Cell proliferation was assayed with a Cell Counting Kit-8 (CCK-8) (Boster, Wuhan, China) according to the manufacturer's instructions. Absorbance was measured by using a microplate reader (Thermo Fisher Scientific, Inc.) at a wavelength of 490 nm.

Apoptosis analysis

To measure apoptosis, a FITC Annexin V apoptosis detection kit I (556547; BD Pharmingen) was used according to the manufacturer's instructions. The cells were stained with Annexin V/PI and detected with flow cytometry. All flow cytometry data were analyzed with FlowJO software.

Cell osteogenesis analysis

To investigate the effects of rifapentine on the osteogenesis of ASCs, cells were digested, harvested, and seeded in 96-well plates at 3,500 cells/well. The alkaline phosphatase (ALP) activity was assayed using an ALP kit (Nanjing Jiancheng Biological Engineering Co. Ltd., Nanjing, China) according to the manufacturer's instructions. Briefly, the cells were washed twice with PBS and lysed with Triton X-100. The lysates were clarified by centrifugation and the supernatant was employed for evaluation. The absorbance of the samples at 520 nm was measured using a microplate reader (Thermo Fisher Scientific, Inc.) on days 3, 7, and 14. The content of ALP was expressed as King unit/100 mL.

Construction of different composites

The HA/TCP (Berkeley Inc.) composite with dimensions of 10×10×3 mm^3 was sterilized by epoxyethane gas. The four composites were constructed according to the different conditions for ASCs culture, and each experimental group was seeded at 4.0×10^4 cells/composite. In brief, ASCs and RPMs were resuspended in solution at designated concentration and drug content (Table 1), and then the suspensions were carefully seeded into each group. The growth medium was added into each well to immerse the specimens completely followed by culturing in a humidified incubator with 5% CO_2 at 37°C. On day 2, the growth medium was replaced with the osteogenic differentiation medium as described earlier. The growth medium was changed every 2 days.

Cell proliferation, osteogenesis, and gene expression in different composites

Cell proliferation analysis

Cell proliferation was assayed with a CCK-8 kit (Dojindo, Kumamoto, Japan) according to the manufacturer's instructions. Cell cultures were prepared in plates as described earlier. At 3, 7, 14, and 21 days of incubation, substrates were

Table 1 The conditions in four experimental groups

Group	RPM	Seeding condition	Abbreviation
A	Without	Monolayer (2D)	ASC
B	With 3 mg RPM	Monolayer (2D)	ASC + RPM
C	Without	Three-dimension (3D)	ASC + HA/TCP
D	With 3 mg RPM	Three-dimension (3D)	ASC + RPM + HA/TCP

Abbreviations: ASC, adipose-derived mesenchymal stem cell; RPMs, rifapentine polylactic acid microspheres; HA/TCP, hydroxyapatite/tricalcium phosphate; 2D, two-dimensional; 3D, three-dimensional.

rinsed with PBS and CCK-8 proliferation kit reagents were added and incubated for 1 hour. Reagents were transferred to 96-well plates, and OD was measured at 450 nm using a microplate reader (Thermo Fisher Scientific, Inc.).

Cell osteogenesis analysis

The ALP activity was assayed using an assay kit (Beyotime, Shanghai, China). Composites were washed twice with PBS and trypsinized for few minutes to detach the cells. Different volumes of standard solution were added into the 96-well plate. Samples (50 μL) were transferred to 96-well plates, and then 50 μL of substrate was added to the well. The plates were incubated at 37°C for 10 minutes. A total of 100 μL of stop solution was added to terminate the reaction. The OD at 405 nm was measured using a microplate reader (Thermo Fisher Scientific, Inc.) on days 3, 7, 14, and 21. The content of ALP was expressed as King unit/mL. The mineralized nodule formed by ASCs in 2D composite (ASC + RPM) was evaluated using Alizarin red staining on day 21.

Gene expression analysis

Quantitative real-time PCR (RT-PCR) was performed to investigate the expression of osteocalcin (OCN) and osteopontin (OPN) on days 14 and 21. The complementary DNA was prepared from total RNA (1 μg) using AccuPower RT PreMix (Perfect Real Time, TaKaRa, China). RT-PCR used SYBR Green PCR Master Mix (Thermo Fisher Scientific, Inc). The adopted primer sequences are as follows: OCN-forward (5′-TTGGTGCACACCTAGCAGAC-3′), OCN-reverse (5′-ACCTTATTGCCCTCCTGCTT-3′); OPN-forward (5′-GAGGGCTTGGTTGTCAGC-3′), OPN-reverse (5′-CAATTCTCATGGTAGTGAGTTTTCC-3′); and GAPDH-forward (5′-ACTTTGTCAAGCTCATTTCC-3′), GAPDH-reverse (5′-TGCAGCGAACTTTATTGATG-3′). PCR amplification and detection were performed on Real-Time Thermal Cycler (Thermo Fisher Scientific, Inc.).

In vitro release test

The concentration of rifapentine in the media of 3D composites (ASCs + RPM + HA/TCP) was measured by high-performance liquid chromatography (HPLC; Shimadzu). Culture solutions were collected and replaced with fresh solutions carefully every 2 days, followed by centrifugation at 10,000× *g* for 5 minutes. Methanol (1 mL) was then added, and the sample was centrifuged at 10,000× *g* for 10 minutes at 4°C. The samples were then ready for analysis. The release rates and cumulative release profiles were calculated and mapped.

Scanning electron microscopy observation

The biocompatibility of 3D composites was directly observed by SEM after culture for 10 days. Briefly, the samples were fixed in 2.5% glutaraldehyde overnight and freeze-dried, and then coated with gold at a thickness of 5 nm and examined by SEM.

H&E staining

The collected samples (10 days after culture) were fixed in paraformaldehyde overnight, and then dehydrated in graded ethanol and embedded in paraffin wax. Sections of 5 μm thicknesses were cut from the paraffin-embedded samples, followed by staining with H&E. The samples were examined under a light microscope.

Statistical analysis

All experiments were conducted in triplicate at least three times. Results are expressed as mean ± SD. Statistical analyses were performed using the SPSS 17.0 software. One-way ANOVA with Tukey's test was employed for the comparisons among groups. A value of $P<0.05$ was considered statistically significant.

Results

Morphology and features of ASCs

ASCs reached 80%–90% confluence and then were passaged every 3 days up to tenth passage without morphologic alteration. ASCs displayed fibroblast-like shape and homogenous and vortex-like growth in monolayers (Figure 1A). Cell cycle analysis revealed that the percentage of P3 ASCs in quiescent phase of G_0/G_1 was 83.35%±3.2% (Figure 1B), with typical

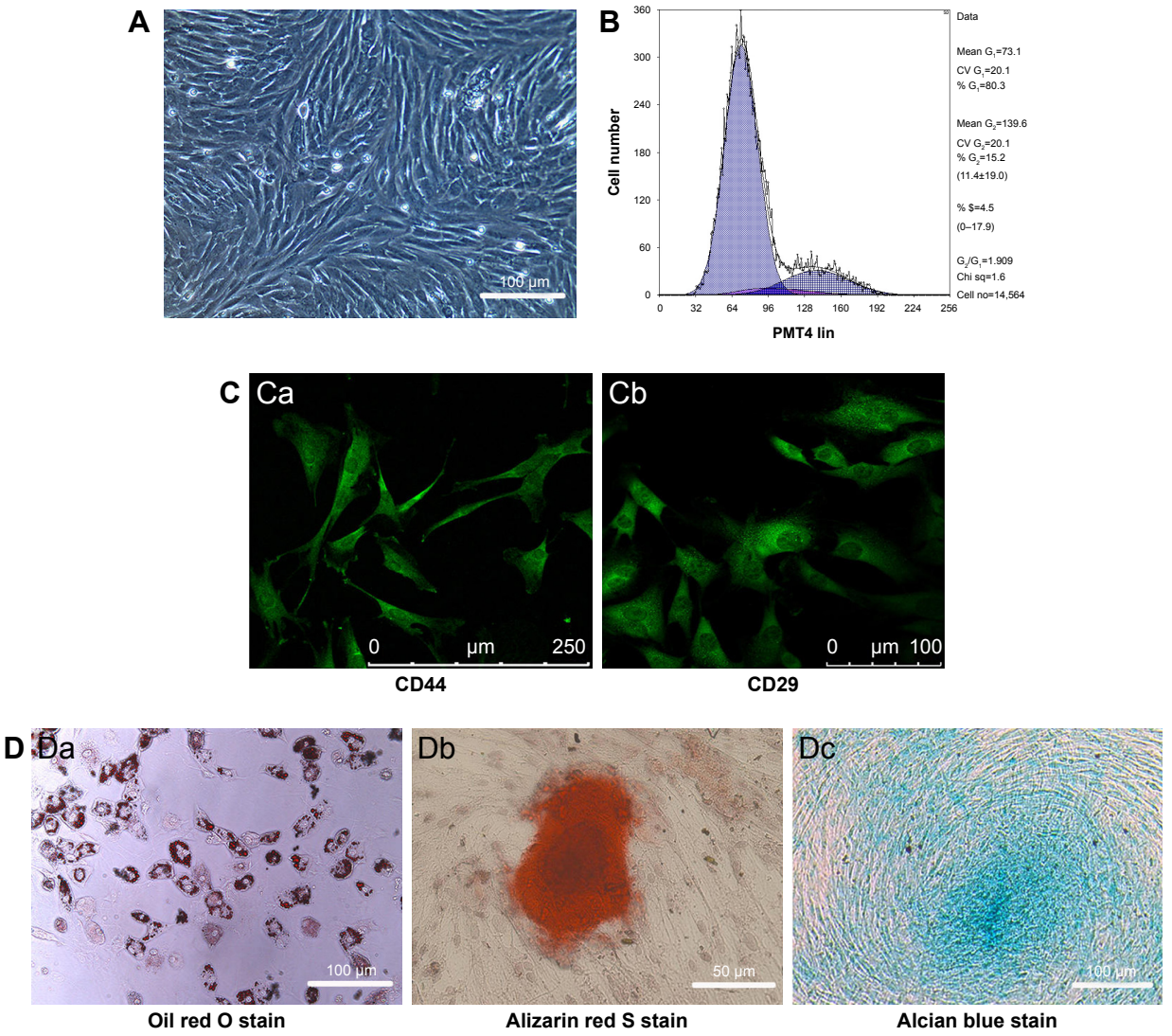

Figure 1 Morphology and features of ASCs.
Notes: (**A**) ASCs displayed fibroblast-like shape and were homogenous. (**B**) Cell cycle analysis revealed that the percentage of P3 ASCs in quiescent phase of G_0/G_1 was 83.35%±3.2%. (**C**) Immunofluorescence staining showed that ASCs expressed the antigens CD44 (Ca) and CD29 (Cb). (**D**) Adipogenic, osteogenic, and chondrogenic differentiation of ASCs and staining with Oil red O (Da), Alizarin red (Db), and Alcian blue (Dc), respectively.
Abbreviations: ASCs, adipose-derived mesenchymal stem cells; P3, passage 3.

stem cell proliferation characteristics. Immunofluorescence staining showed that ASCs expressed the antigens CD44 and CD29 (cytoplasm was stained green) (Figure 1C). ASCs cultured in osteogenic medium for 21 days formed mineral deposits as demonstrated by positive Alizarin red staining. After induction for 7 days in adipogenic medium, Oil Red O staining showed that lipid droplets formed in the cytoplasm. The differentiation to cartilage was reflected by positive Alcian blue staining (Figure 1D).

Morphology and features of RPMs

The RPMs were well dispersed and spherical in shape, and showed smooth surface without hollows or deformations (Figure 2A and B). The mean diameter of the RPMs was 26.4±3.6 µm. The drug loading and encapsulation efficiency were 40.56%±2.63% and 70.24%±2.18%, respectively.

Influence of rifapentine on ASCs

We determined the proliferation of ASCs treated with rifapentine using CCK-8 assay. Cell proliferation rate decreased significantly in the experimental group 4 (30 µg/mL rifapentine) when compared with the control group (0 µg/mL rifapentine) and other groups (10 µg/mL and 20 µg/mL rifapentine) after 4 days (Figure 3A). As mentioned earlier, group 4 (30 µg/mL rifapentine) inhibited ASC growth; then we speculated whether rifapentine at this concentration also induced cell apoptosis. After treatment for 48 hours, we observed increased percentage of early apoptotic cells as well

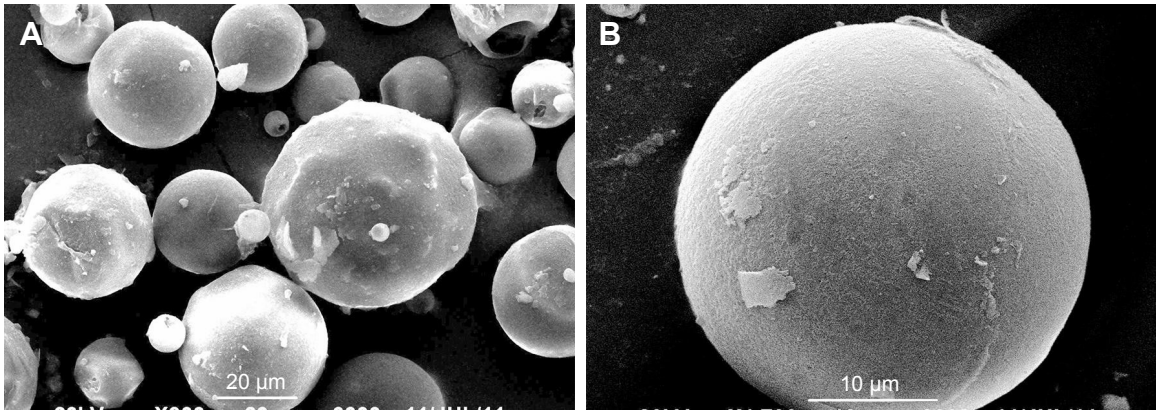

Figure 2 Morphology and features of RPMs.
Notes: SEM images showed the RPMs were spherical in shape and had a smooth surface without protrusions or concaves. (**A**) 1,000× magnification, scale bar =20 μm; (**B**) 2,000× magnification, scale bar =10 μm.
Abbreviations: RPMs, rifapentine polylactic acid microspheres; SEM, scanning electron microscope.

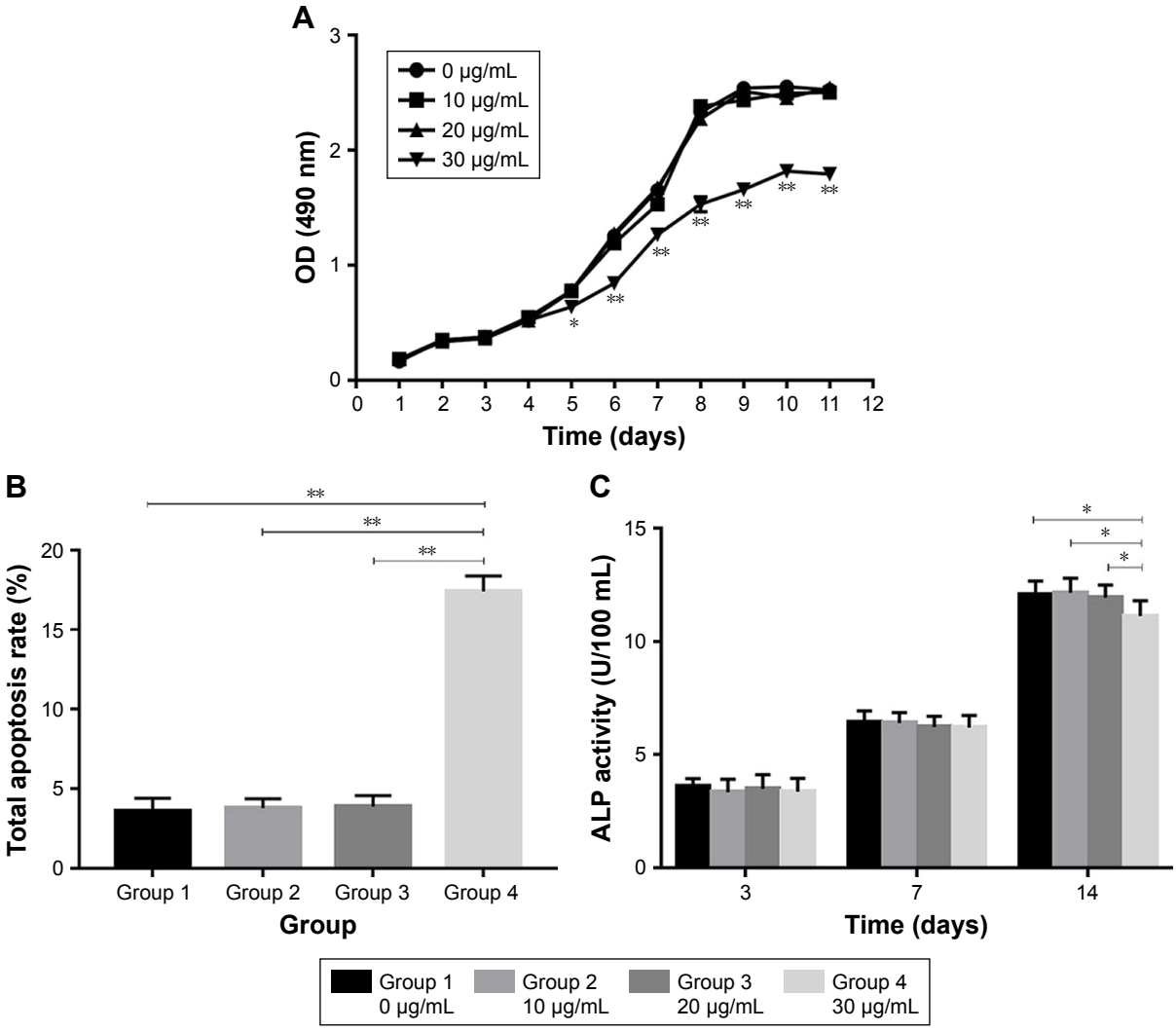

Figure 3 Influence of rifapentine on ASCs.
Notes: (**A**) Cell proliferation rate decreased significantly in group 4. (**B**) The percentage of apoptotic cells increased in group 4. (**C**) The ALP activity gradually increased with the increase of induction time, but the content of ALP in group 4 was lower than other groups on day 14. (*$P<0.05$ and **$P<0.01$).
Abbreviations: ALP, alkaline phosphatase; ASCs, adipose-derived mesenchymal stem cells.

as the late apoptotic cells in group 4 (Figure 3B). Consistent with the CCK-8 assay, the results revealed that rifapentine at the concentration of 30 μg/mL induced cellular apoptosis. Similarly, microplate reader measurements showed that the ALP activity gradually increased with the increase of induction time, but the content of ALP in group 4 was lower than the other three groups on day 14 (Figure 3C).

Cell proliferation, osteogenesis, and gene expression in different composites

Cell proliferation analysis

The proliferation of ASCs in different composites was analyzed by CCK-8 assay (Figure 4A). The ASC proliferation rate increased with incubation time under all conditions. However, cell proliferation in the 2D composites was higher than in 3D composites on days 7, 14, and 21 ($P<0.05$). In 2D composites, proliferation of cells cultured with RPMs was higher than in cells without on day 7 ($P<0.05$). Similarly, proliferation of cells cultured with RPMs in 3D composites was higher than in cells without on days 14 and 21 ($P<0.05$).

Cell osteogenesis analysis

The ALP activity of ASCs increased with incubation time in all experimental groups. In most cases, ALP activity in the 3D composites was higher than in the 2D composites ($P<0.05$ on days 7, 14, and 21; Figure 4B).

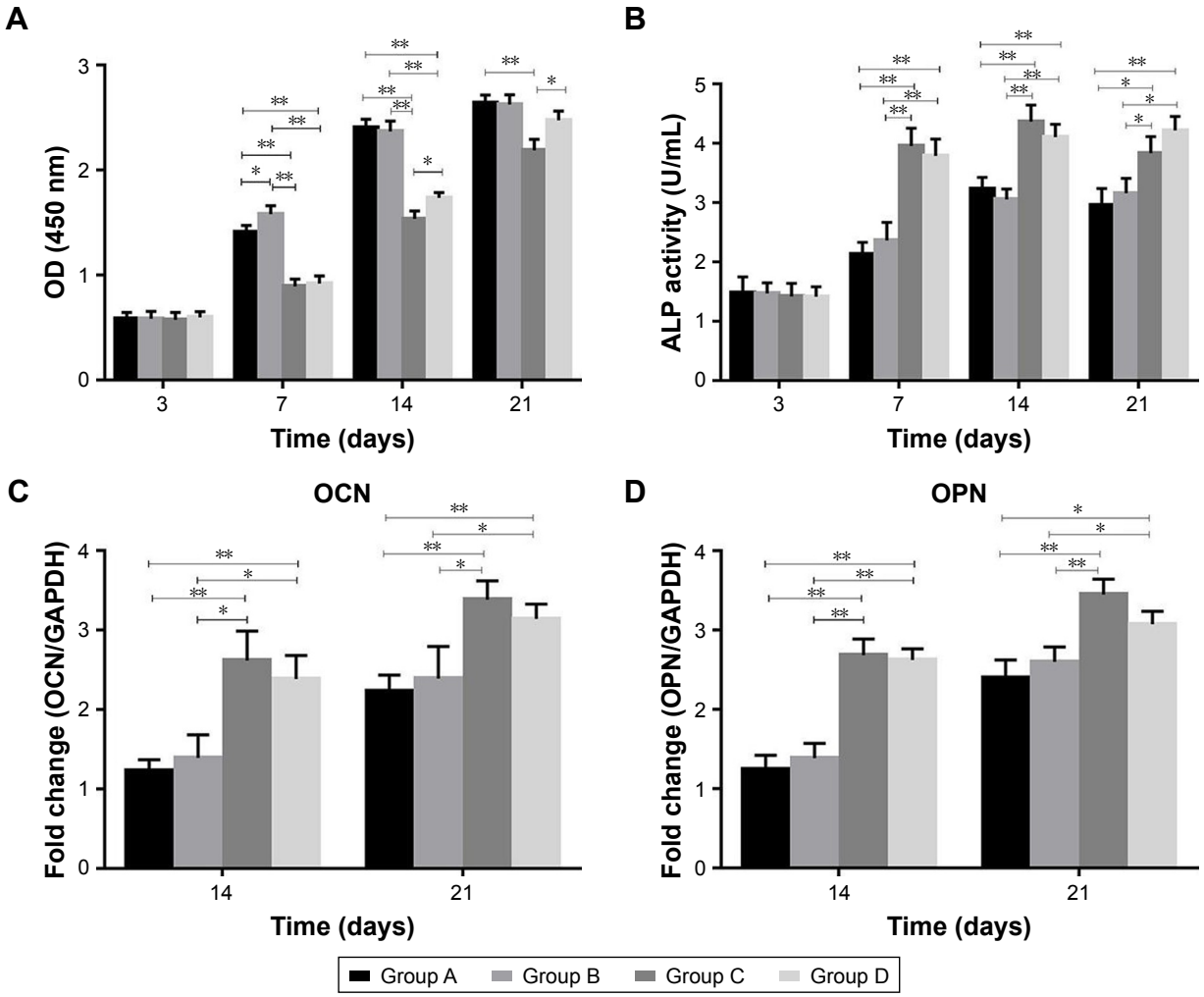

Figure 4 Cell proliferation, osteogenesis, and gene expression in different composites.
Notes: (**A**) The ASC proliferation rate in the 2D composites was higher than in the 3D composites. The proliferation of cells cultured with RPMs was higher than that without on day 7 in 2D composites and on days 14 and 21 in 3D composites, respectively. (**B**) In most cases, ALP activity in the 3D composites was higher than that in 2D composites. (**C**, **D**) The expression of OCN and OPN was upregulated in both 3D and 2D composites, but was higher in 3D composite than in 2D composite (*$P<0.05$ and **$P<0.01$).
Abbreviations: ALP, alkaline phosphatase; ASCs, adipose-derived mesenchymal stem cells; OCN, osteocalcin; OPN, osteopontin; RPM, rifapentine polylactic acid microsphere; 2D, two-dimensional; 3D, three-dimensional.

Gene expression analysis

The expression of OCN and OPN was upregulated in both 3D and 2D composites, but the expression was higher in the 3D composite than in the 2D composite. Furthermore, OCN and OPN expression was not significantly different between RPM groups (groups B and D) and non-RPM groups (groups A and C) (*$P<0.05$ and **$P<0.01$) (Figure 4C, D).

Microscopic image and H&E stain results

Morphological features of 2D composite showed attachment of ASCs to RPMs on the second day of culture. ASCs in 2D composite exhibited elongated fibroblast-like morphology (Figure 5A). Alizarin red staining showed the presence of deposition of mineralized matrix in 2D composites (ASC + RPM) after 21 days of osteogenic incubation. The depositions were surrounded by numerous ASCs and several RPMs. The light-permeable interspaces at the edge of the RPMs indicate the gradual degradation and erosion of microspheres (Figure 5B). The surface of HA/TCP was observed by SEM (Figure 5C). On the tenth day of complex culture of ASCs and HA/TCP, scafflod surface was covered completely by ASCs, and cells stretched like a shuttle and fused to attain membrane shape (Figure 5D). The ultrastructural imaging of 3D composite by SEM showed the RPMs and ASCs tightly adhered to the surface of the scaffold. The cells have a stratiform, elongated morphology, capable of stretching across areas between microspheres and scaffold. Since the time for observation was already 10 days after culture, latticed concaves were observed on the surface of RPMs, which indicated the process of gradual degradation and erosion (Figure 5E, F). Further analysis by H&E stain also showed the porous nature of the RPMs and stretching nature of the ASCs, which enables the ASCs to attach to microspheres and scaffold (Figure 5G).

In vitro release test results

The 2D (ASCs + RPM) and 3D composites (ASCs + RPM + HA/TCP) in our tests exhibited a similar biphasic release profile. A large amount of rifapentine was released during the first 4 days in the 2D composite, which was followed by a period of decreased release rate for 62 days. In the 3D composite, the release kinetics showed a moderate burst release in the first 8 days followed by sustained release for 76 days. At the end of the in vitro release tests, the cumulative release percentages of rifapentine were 88.91%±1.06% for 3D composites and 91.79%±1.14% for 2D composites (Figure 6A and B). The concentration of rifapentine in culture medium was kept below 20 μg/mL at all times.

Discussion

Low drug concentration in the TB lesion, bone defects after removal of osseous tissue, or nonunion after bone graft are major problems that occur in the course of treating osteoarticular TB. At present, the traditional oral or intravenous anti-TB agents combined with debridement or bone transplantation do not result in satisfactory treatment, due to poor blood supply in the necrotic tissues and low osteogenic activity in the transplanted bone. Thus, the combination of drug-delivery system and bone tissue repair appears to be the most promising option for osteoarticular TB treatment. In this study, we developed a novel composite scaffold which allows the controlled release of rifapentine and promotes bone formation simultaneously.

The use of osteogenic stem cells to reconstruct bone tissue is one of the important principles in bone tissue engineering. Adipose tissue is an attractive cellular source of autologous stem cells for regenerative therapies. As one kind of the most promising osteogenic stem cells, the ASCs are much more easily harvested in high yield using simpler, less expensive, and less invasive procedures with a lower incidence of donor site morbidity. As an autologous cell-based therapy, ASC transplants have been successfully used in both soft tissue and bone regeneration. Besides, the excised adipose contains 100–1,000 times more pluripotent cells per cubic centimeter than bone marrow.[13]

We hypothesized that the embedded ASCs in 3D composite will promote bone formation. However, to the best of our knowledge, no previous detailed investigation has evaluated the possibility of combining ASCs and anti-TB drugs. Thus, we cultured the ASCs with varying concentrations of rifapentine to detect the effects of rifapentine on ASC proliferation and osteogenesis. The results showed that rifapentine has no influence on ASC proliferation and osteogenesis when the concentration of rifapentine was below 20 μg/mL, which was significantly higher than the MIC. This result not only makes the combination of 3D composite possible, but also suggested that the concentration of rifapentine should be kept below 20 μg/mL in future experiments.

At present, the traditional oral anti-TB agents do not result in satisfactory treatment of osteoarticular TB, due to the low drug concentration achieved locally in the TB lesion and a series of side effects.[3,7] Because musculoskeletal diseases lack targeting drug delivery systems, drugs cannot be delivered to a specific region;[14] the clinical application of anti-TB drugs to local areas has been shown to be effective after the removal of the bone lesion. However, because the drugs like streptomycin or isoniazid are highly water soluble, they are dissolved and absorbed quickly after being implanted

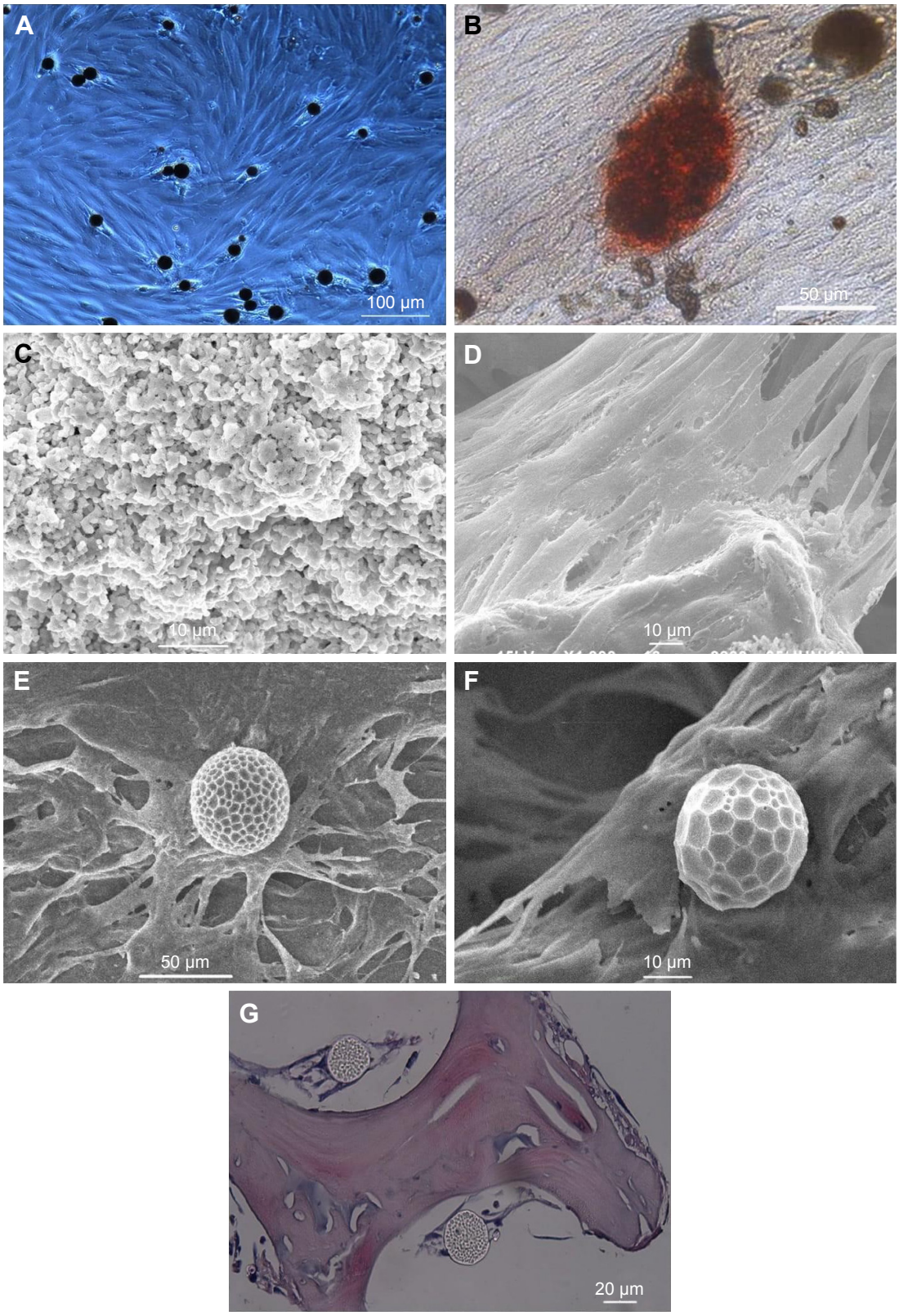

Figure 5 Microscopic image and H&E stain results.

Notes: (**A**) Morphological features of 2D composite shows the attachment of ASCs to RPMs. (**B**) Alizarin red staining shows the presence of mineralized nodule in 2D composite (ASC + RPM) after 21 days of osteogenic incubation. (**C**) SEM results show the surface of HA/TCP. (**D**) On the tenth day of complex culture of ASCs and HA/TCP, the scafflod surface has been covered completely by ASCs, cells stretch like a shuttle and fuse into membrane shape. (**E**, **F**) SEM images showed the RPM and ASCs are tightly adhered to the surface of HA/TCP, and the latticed "concaves" on the surface of RPM indicated the process of gradual degradation and erosion. (**G**) H&E stain also showed the porous nature of the RPMs and stretching nature of the ASCs, which enables the ASCs to attach to microspheres and scaffold.

Abbreviations: ASCs, adipose-derived mesenchymal stem cells; HA/TCP, hydroxyapatite/tricalcium phosphate; RPMs, rifapentine polylactic acid microspheres; SEM, scanning electron microscope; 2D, two-dimensional.

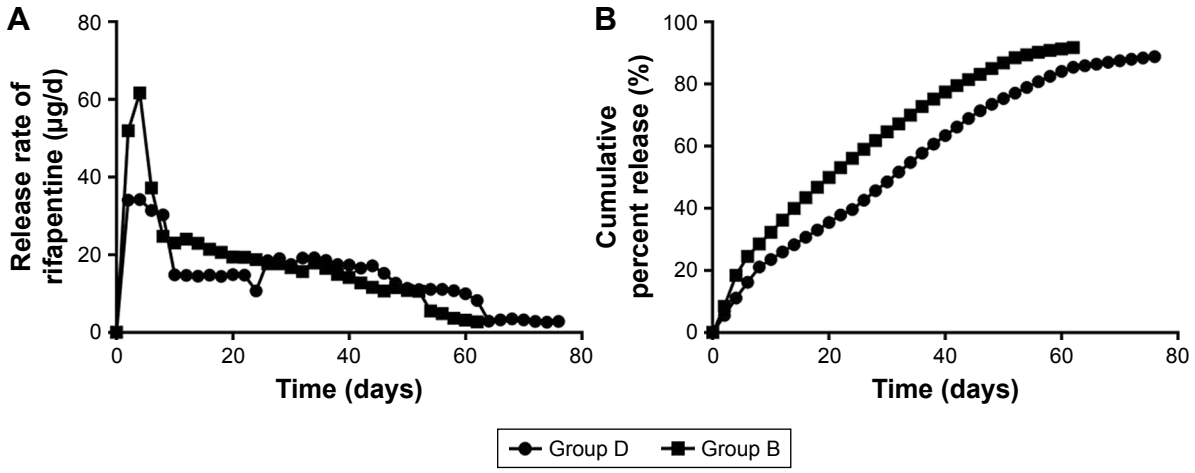

Figure 6 In vitro release test results.
Notes: (**A**) A large amount of rifapentine was released during the first 4 days in 2D composites (ASCs + RPM), which was followed by a period of decreased release rate for 62 days. In 3D composites (ASCs + RPM + HA/TCP), the release kinetics showed a moderate burst release in first 8 days followed by sustained release for 76 days. (**B**) The cumulative release percentages of rifapentine were 88.91%±1.26% for 3D composites and 91.79%±1.49% for 2D composites.
Abbreviations: ASCs, adipose-derived mesenchymal stem cells; HA/TCP, hydroxyapatite/tricalcium phosphate; RPM, rifapentine polylactic acid microsphere; 2D, two-dimensional; 3D, three-dimensional.

during surgery. In contrast, rifapentine has adequate fat solubility and antibacterial properties identical to rifampin. In addition, rifapentine showed a greater inhibitory and bactericidal activity against tubercle bacillus, with a MIC of 0.015–0.06 μg/mL.[10,11]

In recent years, rapid development of microspheres as a drug delivery system has shown great potential for improving TB lesion targeting and reducing toxic side effects of anti-TB drugs.[15] PLA is an ideal material for making microspheres. PLA is a nontoxic, non-irritating, nonimmunogenic, non-carcinogenic material with good biocompatibility and biodegradability.[16] Furthermore, PLA is being used extensively in biomedical applications because of its ability to encapsulate various drug molecules and its sustained release properties.[17] Based on the solubility and stability properties of rifapentine, we used PLA to synthesize the RPMs in our pharmaceutical laboratory. The mean diameter of the RPMs was 26.4±3.6 μm, and the drug loading and encapsulation efficiency were 40.56%±2.63% and 70.24%±2.18%, respectively. The literature review revealed that the drug loading capacity of most rifampicin-loaded PLGA microspheres is relatively low (4.9%–16.5%).[18] Recently, Huang et al[15] fabricated rifapentine-linezolid microspheres for pulmonary TB, and the drug loading and encapsulation efficiency of rifapentine were found to be 18.51%±0.26% and 55.53%±0.78%, respectively. It is obvious that the drug loading and encapsulation efficiency in this study were higher than those mentioned by earlier studies. This improvement could reduce not only the loss of the bioactive substances but also the administration dosage of microspheres. Moreover, the previous study on drug release characteristics and tissue distribution of RPMs in rabbits after paravertebral implantation showed that rifapentine in local vertebral bone tissues was maintained above the MIC for up to 60 days with no apparent accumulation of the drug in other tissues.[7]

However, in bone tissue engineering, microspheres should be combined with scaffolds to maintain local treatment and mechanical strength. In recent years, a wide range of bone tissue engineered scaffolds have been developed to provide better bone graft substitutes for patients. Although the current gold standard for treating the bone defects is autologous bone grafting, it is limited by insufficient tissue supply and donor site morbidity.[19] While using allografts and xenografts may overcome some limitations of the autografts, these bone graft substitutes have the potential risk of immunological rejection and pathogen exposure. In contrast, the HA/TCP composite has been shown to promote bone healing and regeneration due to its excellent osteoinductivity, osteoconductivity, and osteointegration properties.[20] Furthermore, it could be designed to obtain an appropriate shape and size without resulting in any inflammation and rejection following transplantation.[12]

In the present study, RPMs were embedded in HA/TCP composites, and HPLC analyses showed that the duration of release of effective drug concentration was 76 days in a 3D composite, which was longer than that observed in a 2D composite. These results indicated the 3D composites have more obvious sustained release characteristics when compared to 2D composites. The possible causes of prolonged

release were that embedment of RPMs and attachment of ASCs obstructed the release of rifapentine from microspheres. Similar to RPMs, an initial burst of drug release was detected in 2D composites. However, the dual delivery systems were made in 3D composite to adapt these materials to reduce the burst release effect and extend the length of time that rifapentine could be released from the 3D composite, which is more beneficial for local bone tissue absorption of the anti-TB drug. According to literature, controlled drug delivery can be accomplished by physically or chemically adsorbing the drug onto the surface of the scaffold, encapsulating the drug directly within the scaffold, or by incorporating drug delivery systems on the scaffold.[21] Our study used the latter two approaches, which involved the encapsulation of rifapentine in polylactic acid microspheres and then loading these drug-containing microspheres into HA/TCP with the help of ASCs attachment. The integration of microspheres into scaffolds to control the release of drugs in bone tissue engineering applications was similar to the composite hydrogel-microsphere delivery systems reported in cardiac tissue engineering.[22]

The effects of the RPMs in 2D and 3D composites on ASCs proliferation were investigated. The proliferation of ASCs in a monolayer culture was found to be higher than in a 3D composite. The possible causes for a lower rate of cell proliferation in 3D composite were limited diffusion of oxygen and nutrients within the interior of the scaffold. Besides, the cell–cell interaction in 3D composite was different from that in a monolayer, which was likely to influence cell proliferation as well. Compared with 3D composites, cell proliferation in 3D composites plus RPMs was higher and there was significant difference on days 14 and 21. Similar results were found in 2D composites, suggesting that cell proliferation was promoted by RPMs. The reason for the higher proliferation rate in composite containing RPMs could be due to the effects of the PLA. According to the literature, PLA can increase cellular proliferation and attachment.[23] Besides, there were more open and porous structures with the gradual degradation and erosion of RPMs in later stage, leading to more ASCs adhension, which likely improved the proliferation as well.

The 3D composite demonstrated a higher ALP activity than that seen in the 2D composite and suggested a higher degree of early osteogenic differentiation. This results could be explained by the excellent osteoconductive properties of HA/TCP. Osteogenic differentiation was also confirmed by detecting the relative osteogenic gene expression. OCN and OPN are mineralization-related proteins, and their expression will increase after osteoblast differentiation.[24] Similar to ALP activity, the gene expression levels of OCN and OPN in 3D composite were obviously higher than those in 2D composite, suggesting that 3D environment directly enhanced the osteogenic differentiation of ASCs. Furthermore, there was no significant difference between RPM groups and non-RPM groups, which revealed that RPMs have no influence on ASCs osteogenesis.

Conclusion

In this study, we encapsulated rifapentine in polylactic acid microspheres and integrated these microspheres along with rabbit ASCs into HA/TCP made of a dual delivery antituberculotic scaffold for bone tissue engineering. This anti-TB release scaffold has the unique abilities to moderate the burst release, extend the treatment time, and provide a superior 3D environment for ASCs proliferation and osteogenesis. We hope this novel composite scaffold could meet the requirements for treating TB infection, filling bone cavities, and accelerating bone healing. In vivo studies are needed to investigate the effect as an implantation material for regenerating bone defects and releasing anti-TB drug.

Acknowledgment

This work was supported by National Natural Science Foundation of China (grant numbers 81360283 and 81860394).

Disclosure

The authors report no conflicts of interest in this work.

References

1. World Health Organization [webpage on the Internet]. Global tuberculosis report 2018. Available from: http://www.who.int/tb/publications/global_report/en/. Access November 19, 2017.
2. Golden MP, Vikram HR. Extrapulmonary tuberculosis: an overview. *Am Fam Physician*. 2005;72(9):1761–1768.
3. Ge Z, Wang Z, Wei M. Measurement of the concentration of three antituberculosis drugs in the focus of spinal tuberculosis. *Eur Spine J*. 2008;17(11):1482–1487.
4. Zhang HQ, Li JS, Guo CF, et al. Two-stage surgical management using posterior instrumentation, anterior debridement and allografting for tuberculosis of the lower lumbar spine in children of elementary school age: minimum 3-year follow-up of 14 patients. *Arch Orthop Trauma Surg*. 2012;132(9):1273–1279.
5. Jain AK, Dhammi IK. Tuberculosis of the spine: a review. *Clin Orthop Relat Res*. 2007;460:39–49.
6. Wang Y, Wang Q, Zhu R, et al. Trends of spinal tuberculosis research (1994–2015): a bibliometric study. *Medicine*. 2016;95(38):e4923.
7. Zhang Z, Wu L, Li H, Long Z, Song X. Drug release characteristics and tissue distribution of rifapentine polylactic acid sustained-release microspheres in rabbits after paravertebral implantation. *Iran Red Crescent Med J*. 2016;18(11):e38661.
8. Zhang HQ, Lin MZ, Shen KY, et al. Surgical management for multilevel noncontiguous thoracic spinal tuberculosis by single-stage posterior transforaminal thoracic debridement, limited decompression, interbody fusion, and posterior instrumentation (modified TTIF). *Arch Orthop Trauma Surg*. 2012;132(6):751–757.

9. Zhang HQ, Guo CF, Xiao XG, Long WR, Deng ZS, Chen J. One-stage surgical management for multilevel tuberculous spondylitis of the upper thoracic region by anterior decompression, strut autografting, posterior instrumentation, and fusion. *J Spinal Disord Tech*. 2007;20(4):263–267.
10. Mor N, Simon B, Mezo N, Heifets L. Comparison of activities of rifapentine and rifampin against *Mycobacterium tuberculosis* residing in human macrophages. *Antimicrob Agents Chemother*. 1995;39(9):2073–2077.
11. Heifets LB, Lindholm-Levy PJ, Flory MA. Bactericidal activity in vitro of various rifamycins against *Mycobacterium avium* and *Mycobacterium tuberculosis*. *Am Rev Respir Dis*. 1990;141(3):626–630.
12. Hosseinpour S, Ghazizadeh Ahsaie M, et al. Application of selected scaffolds for bone tissue engineering: a systematic review. *Oral Maxillofac Surg*. 2017;21(2):109–129.
13. Arrigoni E, Lopa S, de Girolamo L, Stanco D, Brini AT. Isolation, characterization and osteogenic differentiation of adipose-derived stem cells: from small to large animal models. *Cell Tissue Res*. 2009;338(3):401–411.
14. Fu YC, Fu TF, Wang HJ, et al. Aspartic acid-based modified PLGA-PEG nanoparticles for bone targeting: in vitro and in vivo evaluation. *Acta Biomater*. 2014;10(11):4583–4596.
15. Huang J, Chen Z, Li Y, Li L, Zhang G. Rifapentine-linezolid-loaded PLGA microspheres for Interventional therapy of cavitary pulmonary tuberculosis: preparation and in vitro characterization. *Drug Des Devel Ther*. 2017;11:585–592.
16. Liu X, Liu HY, Lian X, et al. Osteogenesis of mineralized collagen bone graft modified by PLA and calcium sulfate hemihydrate: in vivo study. *J Biomater Appl*. 2013;28(1):12–19.
17. Wischke C, Zhang Y, Mittal S, Schwendeman SP. Development of PLGA-based injectable delivery systems for hydrophobic fenretinide. *Pharm Res*. 2010;27(10):2063–2074.
18. Doan TV, Couet W, Olivier JC. Formulation and in vitro characterization of inhalable rifampicin-loaded PLGA microspheres for sustained lung delivery. *Int J Pharm*. 2011;414(1–2):112–117.
19. Silber JS, Anderson DG, Daffner SD, et al. Donor site morbidity after anterior iliac crest bone harvest for single-level anterior cervical discectomy and fusion. *Spine*. 2003;28(2):134–139.
20. Szubert M, Adamska K, Szybowicz M, Jesionowski T, Buchwald T, Voelkel A. The increase of apatite layer formation by the poly(3-hydroxybutyrate) surface modification of hydroxyapatite and β-tricalcium phosphate. *Mater Sci Eng C Mater Biol Appl*. 2014;34:236–244.
21. Rambhia KJ, Ma PX. Controlled drug release for tissue engineering. *J Control Release*. 2015;219:119–128.
22. Karam JP, Muscari C, Sindji L, et al. Pharmacologically active microcarriers associated with thermosensitive hydrogel as a growth factor releasing biomimetic 3D scaffold for cardiac tissue-engineering. *J Control Release*. 2014;192:82–94.
23. Marei NH, El-Sherbiny IM, Lotfy A, El-Badawy A, El-Badri N. Mesenchymal stem cells growth and proliferation enhancement using PLA vs PCL based nanofibrous scaffolds. *Int J Biol Macromol*. 2016;93(Pt A):9–19.
24. Diefenderfer DL, Osyczka AM, Garino JP, Leboy PS. Regulation of BMP-induced transcription in cultured human bone marrow stromal cells. *J Bone Joint Surg Am*. 2003;85(3):19–28.